

Research Article

Finite element-based validation of infill wall material model for seismic response analysis of reinforced concrete frames



Ridwan^{1*} , Chrisfella Wulandari¹, Yaser Jemaa² , T. Sy. Zahiyyah Aini Wanda Putri¹ , Elsa Attila Salsabila¹ , Enno Yuniarto¹, Alfian Kamaldi¹

ABSTRACT: Masonry infill walls are commonly used in reinforced concrete (RC) frame buildings for both architectural and environmental reasons. Although many consider RC systems to be non-structural, their interaction with surrounding frames can have a significant impact on their lateral stiffness, strength, and seismic performance. This can lead to stiffness issues and soft-story failures during earthquakes. This study looks at the structural function of masonry infills. It compares the experimental load-displacement backbone curve of an infilled RC frame with numerical predictions from four well-known Equivalent Diagonal Strut (EDS) models: Holmes, Mainstone, Liau and Kwan, and Paulay and Priestley. We looked at how well the models performed for both serviceability (initial stiffness) and ultimate limit states (peak lateral strength). The findings demonstrate a definite trade-off in predictive accuracy. With a mean stiffness ratio of 1.38, the Mainstone model yielded the most accurate estimate of elastic stiffness. The Holmes and Liau and Kwan models, on the other hand, significantly overestimated stiffness (ratio = 1.92). All models were conservative (ratios < 1.0) for peak strength. Holmes and Liau and Kwan produced the closest predictions (ratio = 0.84), while Mainstone was the most conservative (ratio = 0.80). These results indicate that the best choice of EDS model depends on the design goal: Mainstone is better for serviceability assessments, while Holmes and Liau and Kwan provide more realistic predictions for ultimate lateral capacity.

Keywords: EDS material model, Infill walls, Seismic response, Initial stiffness, Lateral strength

1. INTRODUCTION

Around the world, reinforced concrete (RC) structures frequently use brick masonry. In addition to acting as architectural partitions, red-brick infill panels offer acoustic and thermal insulation. These panels encounter in-plane forces from the surrounding frame when exposed to seismic forces [1, 2]. Over many years, various experimental and numerical studies have shown that masonry infills can significantly increase the global stiffness and strength of steel and RC frames. They can also alter drift patterns and the overall distribution of damage [3, 4, 5]. However, in design practice, the structural role of infill walls is often ignored. They are treated as non-structural elements [5, 6, 7].

Recent research indicates that this simplification of modelling could lead to an incorrect assessment of seismic behaviour. The placement and distribution of infill walls can significantly affect lateral response. Sometimes, they create vertical irregularities that change torsional behaviour and promote soft-story mechanisms. This increases the risk of collapse [7, 8]. These findings highlight the need for improved representation of masonry infills in structural analysis, especially for buildings that may experience strong ground motions.

Several factors influence the mechanical contribution of brick infill panels. These include the size and arrangement of openings, the quality of the frame-wall connection, and the material properties of the bricks and mortar. Experimental results consistently show that openings reduce the stiffness and strength of infills.

OPEN ACCESS

Affiliation

¹Dept. of Civil Engineering, Universitas Riau, Pekanbaru, Riau, Indonesia, 28293.

²Dept. of Civil Engineering, Liverpool John Moores Univ., Liverpool L3 3AF, United Kingdom

*Correspondence

Email: ridwan@eng.unri.ac.id

ORCID

Ridwan: 0000-0002-4582-0251

Yaser Jemaa: 0000-0001-6313-6528

T. Sy. Zahiyyah Aini Wanda Putri: 0009-0002-9747-9910

Elsa Attila Salsabila: 0009-0003-5067-6690

Received: November 23, 2025

Revised: December 11, 2025

Accepted: December 26, 2025

How to cite: Ridwan, Wulandari, C., Jemaa, Y., Putri, T., Sy., Z., A., W., Salsabila, E., A., Yuniarto, E., Kamaldi, A., (2026). Finite element-based validation of infill wall material model for seismic response analysis of reinforced concrete frames. *Journal of Applied Materials and Technology*, 7(2), 58–65. <https://doi.org/10.31258/Jamt.7.2.58-65>

Copyright (c) 2026 Ridwan, Chrisfella Wulandari, Yaser Jemaa, T. Sy. Zahiyyah Aini Wanda Putri, Elsa Attila Salsabila, Enno Yuniarto, Alfian Kamaldi. This article is licensed under a [Creative Commons Attribution 4.0 International License](https://creativecommons.org/licenses/by/4.0/).



Their effect is closely related to the geometry and placement of the openings [9, 10, 11]. The connection between the frame and the masonry is also important. A strong bond improves load transfer compared to weak or unbonded connections [11, 12]. Furthermore, the strength and flexibility of the units and mortar dictate the main failure modes, while the wall aspect ratio and vertical loading conditions affect the overall response of the system [10, 11, 12, 13].

To understand these complex mechanisms, researchers have developed various modelling strategies. Advanced finite element (FE) micro-models directly replicate mortar joints, interfaces, and masonry units. This makes it possible to accurately replicate bond-slip, cracking, and crushing behaviour under cyclic loading [4, 11, 14]. Simplified macro-models use combined shell-spring representations, nonlinear springs, or equivalent diagonal struts for larger studies. These options allow for better computation. They work well in probabilistic or parametric analyses [14, 15]. Recent FE studies show that predicted stiffness, drift demands, and damage progression are strongly influenced by the opening representation, interface modelling, and specific cyclic constitutive laws [8, 15, 16].

In parallel with FE research, analytical and semi-empirical methods have been improved to make infill modelling more practical for seismic design and assessment. Improvements to diagonal-strut and multi-spring formulations include partial interaction, stiffness reduction, opening corrections, and adjustments based on aspect ratios. These improvements better match laboratory data while maintaining computational efficiency [4, 11, 17]. Simple models have been effectively used in parametric studies that look at variations in mortar strength, wall shape, and vertical loading. They have also been used to assess retrofit methods such as connection strengthening or local jacketing. However, each method has its drawbacks. Micro-models require high computational resources. Macro-models cannot fully capture localised cracking or debonding. Continuum constitutive laws struggle with the natural variability and directionality of masonry [9, 13, 17, 18, 19].

These limitations show the need for modelling methods that balance accuracy and efficiency in describing the nonlinear behaviour of masonry infills during seismic loading. Although many material models have been proposed, there remains uncertainty about how they compare and how they affect overall response predictions. This study compares different material models for masonry infills within RC frames. The goal is to clarify how various models affect stiffness estimation and lateral load capacity during cyclic loading. This will provide a solid basis for choosing appropriate modelling strategies to assess seismic risk and design retrofits for infilled RC frames.

2. METHODOLOGY

A quantitative research approach is used in this study, applying numerical structural analysis through computer-based modelling. The investigation focuses on model verification to find the mechanical properties of brick masonry, which will serve as input parameters for SeismoStruct software. During the verification process, simulation outputs are compared with previously published experimental results to ensure consistency and accuracy. The experimental benchmark selected for this validation is based on the

work of Pallarés et al. [20].

Several experimental programs have examined the behaviour of masonry-infilled RC frames under cyclic loading. This includes studies by Mehrabi et al. [21], Teguh [22] and Pallarés et al. [20]. Although all three investigations evaluated the seismic response of infilled RC systems, they differed in scale, purpose, and specimen layout. Mehrabi et al. [21] conducted tests on 12 half-scale specimens to compare the effects of infills on RC frames designed for wind versus seismic demands. Teguh [22] studied non-engineered construction practices. He focused on the differences in stiffness and ductility between confined clay brick and confined concrete block infills. Meanwhile, Pallarés et al. [20] performed full-scale tests on frames with typical double-wythe masonry façades. Their main goal was to calibrate an equivalent diagonal strut model for seismic evaluation.

Pallarés et al. [20] performed two full-scale tests on 5×3 m RC frames to investigate the effect of masonry façade infills on building seismic behaviour. The test specimens incorporated a conventional Mediterranean double-wythe masonry façade composed of two leaves of hollow, perforated clay brick placed within the RC frame. Under reversed cyclic horizontal displacements, the experiments quantified the infill's contribution to lateral stiffness and ultimate strength. Test data were then used to calibrate a simplified equivalent diagonal-strut macro-model, with the overarching aim of developing a practical, quantitative procedure to account for infill effects in routine seismic design; this calibrated model was subsequently applied to the seismic assessment of a prototype building damaged during the 2011 Lorca earthquake.

2.1. Validated material model. The Equivalent Diagonal Strut (EDS) model is one of the most widely used methods for representing the in-plane stiffness of masonry infill walls in RC frame structures. This method shows the infill as one or more diagonal compression struts that span the beam and column interface. The effective strut width and stiffness come from geometric and material parameters like wall thickness, aspect ratio, and the contact length between the frame and the infill [23, 24]. Recent research has expanded these formulations to consider openings, differences in masonry unit strength (such as strong versus weak bricks), and the properties of the mortar and unit interface. These factors significantly impact the strut's behaviour, predicted capacity, and main failure modes [3, 8]. The EDS expressions adopted in this study are summarised in Table 1, and the corresponding parameters are explained in Figure 1.

2.2. Modelling approach. Columns and beams were represented using the 3D force-based inelastic frame element (infrm-FB in Figure 2) implemented in SeismoStruct. This force-based beam-column element models space-frame members, including both geometric and material nonlinearities. The section response is obtained by integrating the nonlinear uniaxial behaviour of discrete fibres into which the cross-section is subdivided, thereby capturing the distribution of inelasticity both along the member length and through the section depth.

Figure 3 shows a material model for the infill wall in SeismoStruct. The infill panel was represented using a four-node inelastic masonry panel element. Six strut members idealise each panel: two parallel axial struts along each diagonal to transmit compression/tension between opposite corners, and an additional shear strut that transfers shear between the panel's top and bottom. The

Table 1. Equivalent strut width considered in this study.

Equivalent strut width	References
$\frac{w}{d} = \frac{1}{3}$	Holmes [25]
$\frac{w}{d} = 0.16\lambda_h^{-0.3}$, where $\lambda_h = h \sqrt[3]{\frac{E_m t_w \sin 2\theta}{4E_c I_c h}}$	Mainstone [26]
$\frac{w}{h \cos \theta} = \frac{0.95}{\sqrt{(\lambda_h)}}$	Liau and Kwan [27]
$\frac{w}{d} = \frac{1}{4}$	Paulay and Priestley [23]

Where:

w is width of equivalent strut

d is diagonal infill panel length

λ_h is a dimensionless relative stiffness parameter

E_m is the Elastic Modulus of the masonry

t_w is the thickness of the panel

θ is the angle of the diagonal strut with respect to the beams

$E_c I_c$ is the bending stiffness of the columns, and

h is the height of the infill panel

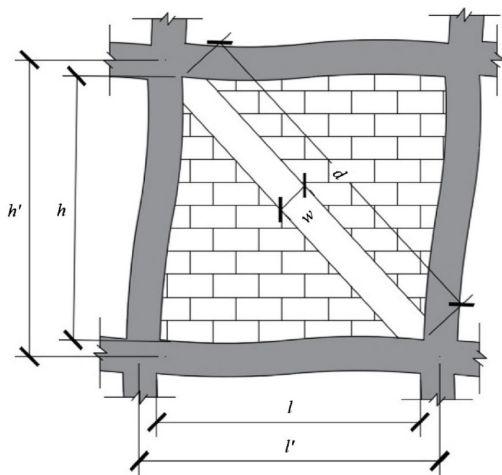


Figure 1. Masonry-infill frame subassemblages [28]

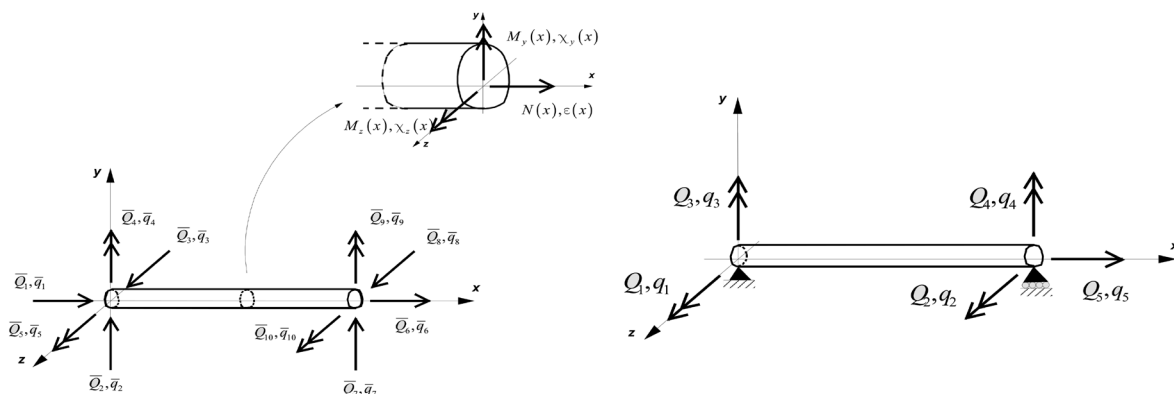


Figure 2. Local axes and output notation for inelastic force-based frame element [29].

shear strut works only on the diagonal when in compression, so its role depends on how the panel deforms. A masonry-strut hysteresis model controls axial struts, while the shear strut follows a specific bilinear hysteretic law. To represent the actual contact shape with the surrounding frame, four internal nodes identify the contact points based on member widths and heights. Additionally, four auxiliary nodes represent the contact length along the frame and infill interface. Internal actions are assembled and mapped to the four exterior element nodes (defined in anti-clockwise order), which provide the connection to the frame.

3. RESULT AND DISCUSSION

This section compares the experimental load-displacement backbone curve obtained from the reversed cyclic tests of Pallarés et al. [20] with four finite-element models that adopt the equivalent diagonal-strut idealisation, using established prescriptions for the strut effective width w from Holmes [25], Mainstone [26], Liao and Kwan [27], and Paulay and Priestley [23]. The experimental backbone curve furnishes a concise measure of the monotonic response of the infilled frame, capturing its stiffness and strength. The observed behaviour may be decomposed into four progressive phases. Stage I exhibits a high, approximately linear elastic stiffness in which the frame and infill behave as a stiff composite system. Stage II begins with a noticeable loss of stiffness as tensile cracking starts in the infill. This usually occurs along the main diagonal or near contact corners. In Stage III, the system reaches its highest capacity (P_{max}) as the diagonal compression mechanism in the infill becomes fully activated. Large compressive forces are then transferred to the bounding frame. Stage IV covers the post-peak deterioration, during which global load capacity falls off rapidly owing to localised damage processes such as corner crushing of the infill, sliding along mortar joints, and possible shear or flexural failures in the surrounding RC members.

3.1. Load-displacement comparison: Experiment VS FE model. The accuracy of the FE models is fundamentally dependent on the formulation used to determine the equivalent strut's effective width (w), which dictates the infill's stiffness contribution. The four models, as shown in Figure 4, yield different predictions for this width, resulting in significant differences in the simulated backbone curves.

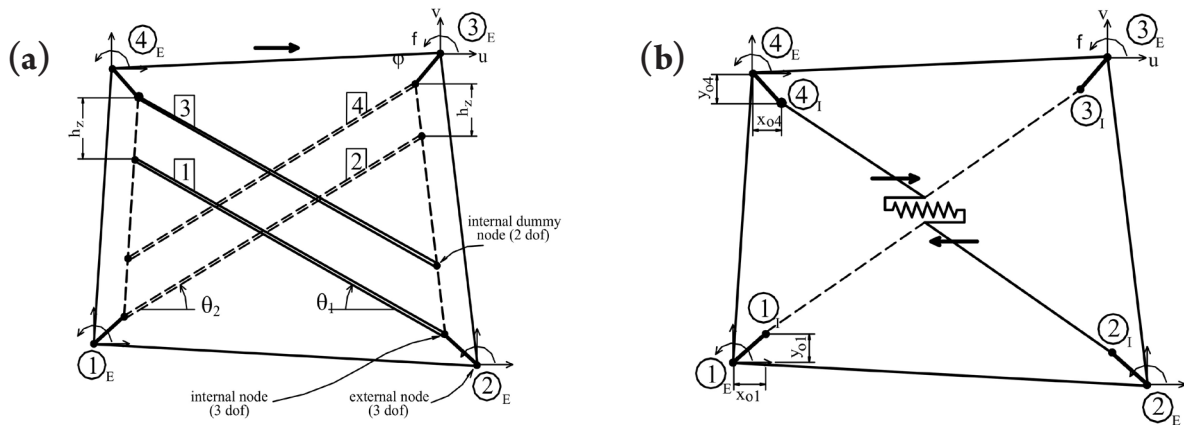


Figure 3. Material models for representing infill wall in RC frames: a) compression/tension struts and b) shear strut analogy [30].

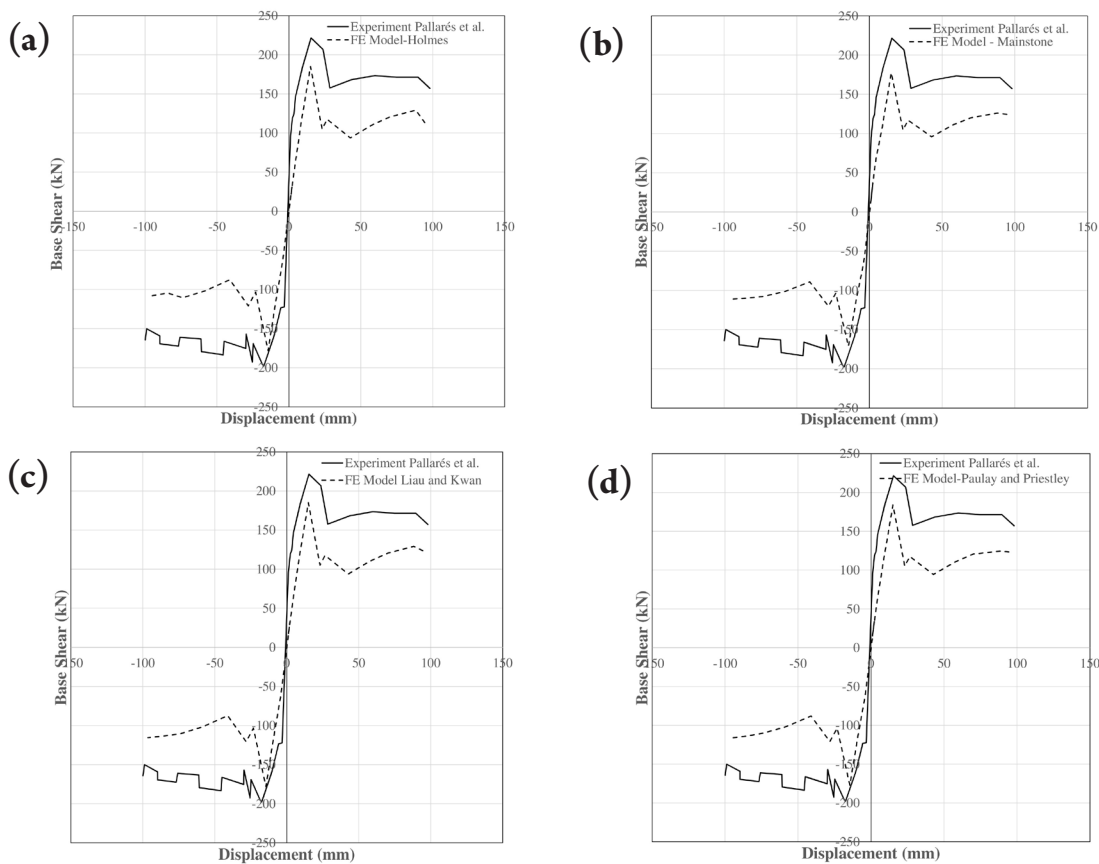


Figure 4. Comparative analysis of the experimental results of Pallarés et al [20] with numerical predictions in this study using EDS Models of (a) Holmes, (b) Mainstone, (c) Liau and Kwan, and (d) Paulay and Priestley

The Holmes model, an early and simplified geometric approach (typically $w = d/3$), often overestimates the composite system's initial stiffness and peak strength. This overestimation is attributed to its inability to fully account for the RC frame's relative flexibility and the resulting separation between the frame and infill elements during loading.

On the other hand, the initial stiffness seen in the experimental results is typically more accurately predicted by the Mainstone model, which incorporates the non-dimensional parameter λ_i (the relative stiffness ratio between the frame and infill). By accounting

for frame-infill interaction, the Mainstone formulation usually provides a better representation of the structure's elastic behaviour than simple geometric models. The models suggested by Liau and Kwan are more complex. They account for different failure modes and the infill panel's aspect ratio. Depending on the primary failure mode observed in the experiment, such as diagonal tension or corner crushing, a well-calibrated Liau and Kwan model can accurately predict the ultimate peak strength.

Finally, the Paulay and Priestley model often assumes a constant strut width ($w = d/4$). This model typically provides a

Table 2. Typical performance of equivalent diagonal strut to the strength characteristics of the infilled frame.

Model	Effective Strut Width (w)	Stage I: Initial Stiffness	Stage III: Peak Strength (P_{max})	General Commentary
Holmes [25]	Simple Geometric ($\approx d/3$)	Overestimates (Too stiff)	Overestimates (Non-conservative)	Simple, tends to ignore frame flexibility.
Mainstone [26]	Relative Stiffness (λ_n)	Superior/Closest Match	Good/Accurate Prediction	Best suited for predicting elastic behavior.
Liau and Kwan [27]	Failure Modes & Aspect Ratio	Good/Accurate Prediction	Most Accurate	Complex, accounts for diverse failure mechanisms.
Paulay & Priestley [23]	Fixed Fraction ($\approx d/4$)	Conservative Estimate (Too flexible)	Conservative Estimate	Simple, often adopted in design codes for safety.

conservative estimate of strength compared to experimental results and models like Mainstone. However, this conservatism is usually viewed as a safe and preferred approach in design practices due to its simplicity and built-in safety margin. To validate the numerical models, a careful comparison was conducted across key response metrics of the backbone curve:

3.1.1. Initial stiffness and peak strength. The analysis of the initial slope (Stage I stiffness) and the maximum lateral load (Stage III, P_{max}) highlights how well the equivalent strut models work. Differences between the experimental and FE curves in Stage I indicate problems with calculating the effective strut width (w) at small displacements. As expected, models that depend on the relative stiffness parameter λ_n , like Mainstone, usually match well with the experimental initial stiffness. For P_{max} , the most accurate FE model is the one whose simulated peak load is nearest to the experimental ultimate capacity ($P_{max}/F_{experiment}$). The Holmes model tends to overestimate P_{max} due to a considerable effective strut width, while the Paulay and Priestley model slightly underestimates it, reflecting the unique nature of these strut formulations.

3.1.2. Stiffness degradation and post-peak response. Simulating post-peak behaviour (Stage IV) is the biggest challenge for macro-models. While the EDS models define initial elastic properties, the degradation rate is influenced by the plastic and damage parameters in the FE software's material model (e.g., Concrete Damage Plasticity). A successful FE model needs a precise strut width, as shown in Mainstone or Liau and Kwan. It also needs damage parameters that reflect the strength loss observed in experiments. If a simulated curve shows a sudden or gradual decrease in strength compared to the experiment, it suggests that material properties, like the ultimate strain capacity of the infill or frame elements, need to be changed. The results emphasise the EDS formulation, which offers the most dependable and realistic simulation of the entire backbone curve of the RC infilled frame. This includes the initial elastic behaviour and the final strength loss.

Table 2 summarises the typical performance of each equivalent diagonal strut model when predicting the stiffness and strength characteristics of the infilled RC frame, based on the influence of their calculated effective strut width (w).

3.2. Mean load ratio comparison ($P_{FE} / P_{Experiment}$). To quantitatively assess model accuracy in predicting ultimate strength (Stage III, P_{max}), the mean load ratio ($P_{FE} / P_{Experiment}$) was calculated for each model. The results, presented in Figure 5, show that all four EDS models provide a conservative estimate of the experimental peak strength. The ideal value for this ratio is 1.0. Since all calculated ratios are less than 1.0, the FE models consistently underesti-

mate the measured experimental load-carrying capacity ($P_{Experiment}$).

The Holmes and Liau and Kwan models both yield the highest mean load ratios at 0.84. This indicates that these models predict a peak strength approximately 16% lower than the experimental result. While conservative, this level of prediction is the closest to the experimental result among the four models, aligning with the qualitative observation that Liau and Kwan are often accurate for ultimate strength.

The Paulay and Priestley model follows closely with a ratio of 0.83, underestimating the strength by 17%. The Mainstone model, despite being the most accurate for initial stiffness (Figure 5), proves to be the most conservative for ultimate strength, yielding the lowest mean load ratio of 0.80 (a 20% underestimation).

This quantitative analysis of peak strength shows that, for this specific experimental setup, all tested EDS models give a safe, conservative estimate of ultimate lateral load capacity. The difference in accuracy is small. The Holmes and Liau and Kwan models perform slightly better at predicting ultimate strength than the Mainstone model. This trade-off between accurately predicting stiffness (Mainstone) and ultimate strength (Holmes and Liau and Kwan) is a common issue when choosing the best equivalent diagonal strut formulation.

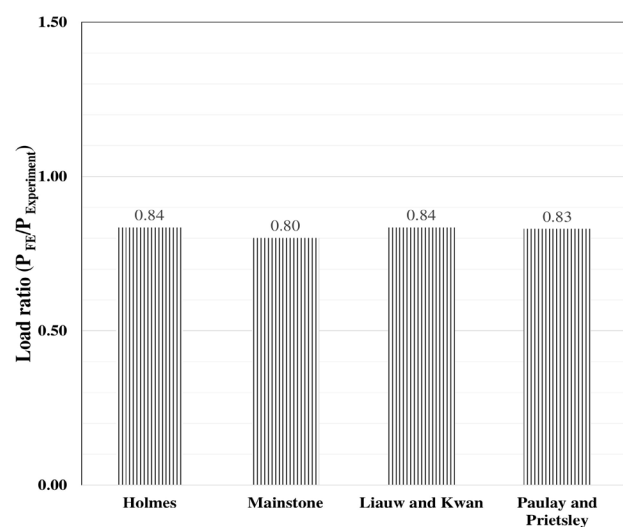
**Figure 5.** Mean load ratio ($P_{FE} / P_{Experiment}$) comparison for the four EDS models.

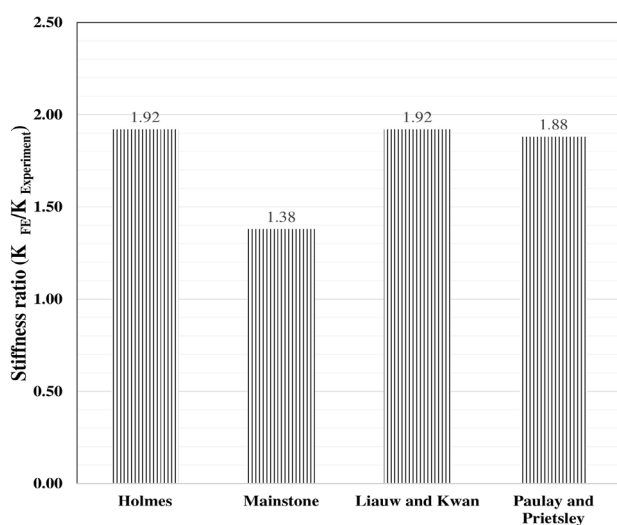
Table 3. Predicting the stiffness and strength characteristics of the infilled RC frame.

Model	Effective Strut Width (w) Basis	Stiffness Ratio ($K_{FE} / K_{Experiment}$)	Load Ratio ($P_{FE} / P_{Experiment}$)
Holmes [25]	Simple Geometric	1.92 (Significant overestimation)	0.84 (Closest to experiment)
Mainstone [26]	Relative Stiffness (λ_h)	1.38 (Most accurate)	0.80 (Most conservative)
Liau and Kwan [27]	Failure Modes & Aspect Ratio	1.92 (Significant overestimation)	0.84 (Closest to experiment)
Paulay & Priestley [23]	Fixed Fraction ($\approx d/4$)	1.88 (High overestimation)	0.83 (Mid-Range conservative)

3.3. Stiffness ratio comparison ($K_{FE} / K_{Experiment}$). To assess model accuracy in predicting the initial elastic behaviour (Stage I stiffness, K), the mean stiffness ratio ($K_{FE}/K_{Experiment}$) was calculated for each model. The results in Figure 6 clearly show the differences in initial stiffness predictions among the four models. The ideal value for this ratio is 1.0, which means a perfect match between the FE model prediction (K_{FE}) and the Experimental result ($K_{Experiment}$).

The Mainstone model has the lowest mean stiffness ratio at 1.38. While this is still an overestimation (the FE model is 38% stiffer than the experiment on average), it is much closer to the ideal 1.0 than the other formulations. This confirms the earlier observation: the Mainstone formulation accurately reflects the relative stiffness of the bounding RC frame and offers the best representation of the structure's initial elastic behaviour.

In contrast, the Holmes and Liau and Kwan models both show mean ratios of 1.92, indicating that these models overestimate initial stiffness by 92%. This overestimation is a known issue with the Holmes geometric model. Liau and Kwan suggest that while the model may predict ultimate strength (P_{max}) accurately, its formula for w might not perform well during the initial elastic phase. The Paulay and Priestley model provides a slightly better, but still greatly overestimated, ratio of 1.88. The quantitative evidence from the stiffness-ratio comparison backs the conclusion that the Mainstone model gives the most accurate and least conservative prediction of the initial elastic stiffness. This is a crucial factor for assessing serviceability limit states in structural design.

**Figure 6.** Stiffness ratio comparison for the four EDS models.

The performance of the four strut models in this study matches the general agreement found in structural engineering literature, particularly in studies that involve quasi-static cyclic testing of infilled frames (e.g., Mehrabi et al., [21]). Usually, the Mainstone model confirms its initial stiffness prediction. Its formula shows the initial contact length and connects strut width to the relative stiffness of the frame. On the other hand, the Holmes model often overestimates strength and stiffness. This overestimation problem is often present in simple geometric models that ignore the distance between the frame and infill. Empirical relations based on failure modes, such as those from Liau and Kwan, or models that consider the flexibility of the frame such as Mainstone, are often found to be more reliable for both elastic and ultimate strength conditions. Assuming a constant $d/4$ width, many studies show that the Paulay and Priestley model gives an average or conservative result in various experiments. This supports its common use in seismic assessment guidelines, such as FEMA 356/ASCE 41, as a safe and simple method instead of providing an exact simulation of a specific test specimen. Thus, the differences among the FE models in this study fit well with the known strengths and weaknesses of each equivalent strut formulation.

Table 3 summarises the stiffness and strength characteristics of the infilled RC frame found in this study. The study's conclusion that the Mainstone model provides the most accurate initial stiffness prediction ($K_{FE} / K_{Experiment} = 1.38$) is often supported in the literature, which reports stiffness ratios of 1.20-1.50 for the Mainstone model when analysing similar infilled RC frames. This supports the idea that the Mainstone model is the best option for serviceability limit state assessments because it includes the relative stiffness of the surrounding RC frame through the λ_h parameter. On the other hand, the Holmes model significantly overestimates initial stiffness. It has a ratio of 1.92. This highlights warnings in the literature about simplified geometric methods that ignore frame flexibility. As a result, it can lead to the assumption of overly stiff, full-contact behaviour.

Regarding ultimate strength, the results align with the literature, which finds that all tested models provide a safe, conservative estimate of the experimental capacity. Specifically, the Liau and Kwan model (ratio of 0.84) provides the closest prediction to the ultimate experimental capacity, consistent with the literature's recognition that its formulation, which considers various failure modes, is often optimised for peak-load assessment. Meanwhile, the Mainstone model's conservative prediction of strength (ratio of 0.80) and the Paulay and Priestley model's mid-range conservative result (ratio of 0.83) are both well within the expected bounds established in the literature for the seismic assessment of infilled frames.

Models that are best for elastic stiffness (like Mainstone) are often the most conservative for ultimate strength, while models designed around the ultimate mechanism (like Liau & Kwan) offer the highest-fidelity predictions for P_{max} . The literature confirms that the Mainstone model (for stiffness) and the Liau and Kwan model (for strength) are generally the most technically accurate, although the Paulay and Priestley model remains popular due to its simplicity and inherent safety margin.

4. CONCLUSION

The comparison of the four EDS models with the experimental backbone curve reveals an important trade-off in predictive accuracy. This depends on the stage of the structural response being modelled. In the early elastic phase, the Mainstone model provides the best simulation of initial stiffness, achieving the lowest mean stiffness ratio ($K_{FE} / K_{Experiment} = 1.38$). This accuracy comes from including the relative stiffness parameter (λ_h), which captures the frame-infill interaction well at low displacements. On the other hand, the geometric-based Holmes model and the failure-mode-based Liau and Kwan models both vastly overestimate the initial stiffness, with ratios of 1.92. This overestimation results from incorrectly estimating the effective strut width (w) in the elastic range.

For the ultimate limit state, all four models yield conservative estimates for the peak lateral load (P_{max}). The Holmes and Liau and Kwan models provided the most accurate prediction of ultimate strength (mean load ratio $P_{FE} / P_{Experiment} = 0.84$), underestimating the experimental capacity by 16%. The Mainstone model, despite its accuracy in stiffness prediction, proved to be the most conservative for strength, underestimating P_{max} by 20% (ratio of 0.80).

Ultimately, the design goal determines which EDS model is best. The Mainstone method is better for serviceability checks that rely on accurate initial stiffness. On the other hand, the Holmes formulations and the Liau-Kwan model usually yield slightly more accurate results when the objective is to estimate ultimate lateral capacity. The Paulay and Priestley model consistently gives safe, mid-range estimates for both metrics, proving its usefulness in simplified design code applications.

ACKNOWLEDGEMENTS

This research was supported by Universitas Riau under grant number 15516/2024. The authors also wish to express their gratitude to the Department of Civil Engineering Universitas Riau for providing the necessary facilities.

CREDIT AUTHOR STATEMENT

Ridwan: Conceptualization, Methodology, Investigation, Formal analysis, Project administration, Supervision, Visualization, Writing—original draft. **Chrisfella Wulandari:** Methodology, Investigation, Formal analysis, Software, Validation, Visualization, Writing—original draft. **Yaser Jemaa:** Software, Supervision, Writing—original draft. **T. Sy. Zahiyyah Aini Wanda Putri:** Methodology, Investigation, Formal analysis, Software, Validation, Visualization, Writing—original draft. **Elsa Attila Salsabila:** Methodology, Investigation, Formal analysis, Software, Validation, Visualization, Writing—original draft. **Enno Yuniarto:** Supervision, Writing—original draft. **Alfian Kamaldia:** Software, Supervision, Writing—original draft.

DECLARATIONS

Conflict of interest The authors declare that they have no known competing financial interests or personal relationships that could have appeared to influence the work reported in this paper.

REFERENCES

- [1] Kim M, Yu E. Experimental study on lateral-load-resisting capacity of masonry-infilled reinforced concrete frames. *Applied Sciences*. 2021;11(21), DOI: <https://doi.org/10.3390/app11219950>.
- [2] Roosta S, Liu Y. Behavior of concrete masonry infills bounded by masonry frames subjected to in-plane lateral loading – Experimental study. *Engineering Structures*. 2021; 247:113153, DOI: <https://doi.org/10.1016/j.engstruct.2021.113153>.
- [3] Messaoudi A, Chebili R, Mohamed H, Rodrigues H. Influence of masonry infill wall position and openings in the seismic response of reinforced concrete frames. *Applied Sciences*. 2022;12(19), DOI: <https://doi.org/10.3390/app12199477>.
- [4] Dhir PK, Tubaldi E, Ahmadi H, Gough J. Numerical modelling of reinforced concrete frames with masonry infills and rubber joints. *Engineering Structures*. 2021;246:112833, DOI: <https://doi.org/10.1016/j.engstruct.2021.112833>.
- [5] Sleiman E, Ferrier E, Michel L, Saidi M. Seismic behavior of masonry-infilled reinforced concrete frames strengthened using ultra-high performance concrete diagonal strips. *Structures*. 2024;59:105790, DOI: <https://doi.org/10.1016/j.istruc.2023.105790>.
- [6] Anić F, Penava D, Guljaš I, Sarhosis V, Abrahamczyk L. Out-of-plane cyclic response of masonry infilled RC frames: An experimental study. *Engineering Structures*. 2021;238:112258, DOI: <https://doi.org/10.1016/j.engstruct.2021.112258>.
- [7] Mazza F, Donnici A. In-plane-out-of-plane single and mutual interaction of masonry infills in the nonlinear seismic analysis of RC framed structures. *Engineering Structures*. 2022; 257: 114076, DOI: <https://doi.org/10.1016/j.engstruct.2022.114076>.
- [8] Usta P, Onat Ö, Bozdağ Ö. Effect of masonry infill walls on the nonlinear response of reinforced concrete structure: October 30, 2020 İzmir earthquake case. *Engineering Failure Analysis*. 2023;146:107081, DOI: <https://doi.org/10.1016/j.engfailanal.2023.107081>.
- [9] Furtado A, Arède A, Rodrigues H, Varum H. The role of the openings in the out-of-plane behaviour of masonry infill walls. *Engineering Structures*. 2021;244:112793, DOI: <https://doi.org/10.1016/j.engstruct.2021.112793>.
- [10] Tripathy D, Singhal V. Experimental and analytical investigation of opening effects on the in-plane capacity of unreinforced masonry wall. *Engineering Structures*. 2024;311:118161, DOI: <https://doi.org/10.1016/j.engstruct.2024.118161>.
- [11] Milijaš A, Marinković M, Butenweg C, Klinkel S. Experimental results of reinforced concrete frames with masonry infills with and without openings under combined quasi-static in-plane and out-of-plane seismic loading. *Bulletin of Earthquake Engineering*. 2023;21(7):3537-79, DOI: <https://doi.org/10.1007/s10518-023-01664-4>.

- [12] Milijaš A, Marinković M, Butenweg C, Klinkel S. Experimental investigation on the seismic performance of reinforced concrete frames with decoupled masonry infills: considering in-plane and out-of-plane load interaction effects. *Bulletin of Earthquake Engineering*. 2024;22(15):7489-546, DOI: <https://doi.org/10.1007/s10518-024-02012-w>.
- [13] Nazimi K, Castro JJ, Omi S, Stanikzai MA. Investigating the compressive strength of clay brick masonry: a case study of Nangarhar, Afghanistan. *Buildings*. 2024;14(12), DOI: <https://doi.org/10.3390/buildings14123882>.
- [14] Mudragada R, Bhargava P. Effect of masonry infill on the response of reinforced concrete frames subject to in-plane blast loading. *Structures*. 2023;57:105317, DOI: <https://doi.org/10.1016/j.istruc.2023.105317>.
- [15] El-Kholy AM, Sayed SM, El-Assaly MM. Nonlinear macromodeling of multistory RC buildings with masonry infill walls. *Bulletin of Earthquake Engineering*. 2024;22(3):1451-84, DOI: <https://doi.org/10.1007/s10518-023-01787-8>.
- [16] İzol R, Işık E, Avcil F, Arslan MH, Arkan E, Büyüksaraç A. Seismic performance of masonry structures after 06 February 2023 earthquakes; site survey and FE modelling approach. *Soil Dynamics and Earthquake Engineering*. 2024;186:108904, DOI: <https://doi.org/10.1016/j.soildyn.2024.108904>.
- [17] Tekeli Kabaş H, Ebrahim Kusain F, Anıl Ö. Experimental behavior of masonry infilled RC frames with openings strengthened by using CFRP strip. *Composite Structures*. 2023; 312:116873, DOI: <https://doi.org/10.1016/j.compstruct.2023.116873>.
- [18] Liguori FS, Madeo A, Formisano A. Seismic vulnerability of industrial steel structures with masonry infills using a numerical approach. *Bulletin of Earthquake Engineering*. 2024;22(2):519-45, DOI: <https://doi.org/10.1007/s10518-023-01794-9>.
- [19] Falcão Moreira R, Varum H, Castro JM. Influence of masonry infill walls on the seismic assessment of non-seismically designed RC framed structures. *Buildings*. 2023;13(5), DOI: <https://doi.org/10.3390/buildings13051148>.
- [20] Pallarés FJ, Davia A, Hassan WM, Pallarés L. Experimental and analytical assessment of the influence of masonry façade infills on seismic behavior of RC frame buildings. *Engineering Structures*. 2021;235:112031, DOI: <https://doi.org/10.1016/j.engstruct.2021.112031>.
- [21] Mehrabi Armin B, Benson Shing P, Schuller Michael P, Noland James L. Experimental evaluation of masonry-infilled RC frames. *Journal of Structural Engineering*. 1996; 122(3):228-37, DOI: [https://doi.org/10.1061/\(ASCE\)0733-9445\(1996\)122:3\(228\)](https://doi.org/10.1061/(ASCE)0733-9445(1996)122:3(228)).
- [22] Teguh M. Experimental evaluation of masonry infill walls of RC frame buildings subjected to cyclic loads. *Procedia Engineering*. 2017;171:191-200, DOI: <https://doi.org/10.1016/j.proeng.2017.01.326>.
- [23] Paulay T, Priestley MJN. *Seismic design of reinforced concrete and masonry buildings*: Wiley New York; 1992.
- [24] Asteris PG, Cotsovos DM, Chrysostomou CZ, Mohebkhah A, Al-Chaar GK. Mathematical micromodeling of infilled frames: State of the art. *Engineering Structures*. 2013;56:1905-21, DOI: <https://doi.org/10.1016/j.engstruct.2013.08.010>.
- [25] Holmes M. Steel frames with brickwork and concrete infilling. *Proceedings of the Institution of Civil Engineers*. 1961; 19(4): 473-8, DOI: <https://doi.org/10.1680/iicep.1961.11305>.
- [26] Mainstone RJ. On the stiffness and strengths of infilled frames. *Proceedings of the Institution of Civil Engineers*. 1971; 49(2): 230-, DOI: <https://doi.org/10.1680/iicep.1971.6267>.
- [27] Te-Chang L, Kwok-Hung K. Nonlinear behaviour of non-integral infilled frames. *Computers & Structures*. 1984;18(3):551-60, DOI: [https://doi.org/10.1016/0045-7949\(84\)90070-1](https://doi.org/10.1016/0045-7949(84)90070-1).
- [28] Wijaya H, Rajeev P, Gad E, Amirsardari A. Effect of infill-wall material types and modeling techniques on the seismic response of reinforced concrete buildings. *Natural Hazards Review*. 2020;21(3):04020031, DOI: [https://doi.org/10.1061/\(ASCE\)NH.1527-6996.0000395](https://doi.org/10.1061/(ASCE)NH.1527-6996.0000395).
- [29] Wijaya Spacone E, Filippou FC, Taucer FF. Fibre beam-column model for non-linear analysis of r/c frames: part i. Formulation. *Earthquake Engineering & Structural Dynamics*. 1996;25(7):711-25, DOI: [https://doi.org/10.1002/\(SICI\)1096-9845\(199607\)25:7<711::AID-EQE576>3.0.CO;2-9](https://doi.org/10.1002/(SICI)1096-9845(199607)25:7<711::AID-EQE576>3.0.CO;2-9).
- [30] Crisafulli FJ, Carr AJ. Proposed macro-model for the analysis of infilled frame structures. *Bulletin of the New Zealand Society for Earthquake Engineering*. 2007;40(2):69-77, DOI: <https://doi.org/10.5459/bnzsee.40.2.69-77>.